Stochastic spatial behaviour in deterministic pattern formation

1990 J. Phys. A: Math. Gen. 23 L259

(http://iopscience.iop.org/0305-4470/23/6/005)

J. Phys. A: Math. Gen. 23 (1990) L259-L264. Printed in the UK

LETTER TO THE EDITOR

Stochastic spatial behaviour in deterministic pattern formation

Viktor K Horváth and Tamás Vicsek

Institute for Technical Physics, Budapest, PO Box 76, 1325 Hungary

Received 8 January 1990

Abstract. We introduce a new approach to the analysis of growing unstable interfaces in order to characterise the degree of their randomness. Highly ramified viscous fingering patterns are digitised and the related surface curvature data are evaluated using techniques common in the investigations of dynamical systems. Our results for the associated correlation dimension indicate that the experimentally observed deterministic patterns correspond to a spatial behaviour which is more complex than a low-dimensional chaotic geometry.

Far from equilibrium growth processes [1-3] such as aggregation [4, 5], electrodeposition [6], solidification [7], dielectric breakdown [8] and viscous fingering [9-11] typically lead to patterns having an apparently random, fractal [12, 13] structure. In most cases this is so even for phenomena where the development of the unstable interface is described by deterministic equations [14]. This fact raises the intriguing question of analogies between temporal chaos and spatial disorder; a question which has been known for some time, but has not been addressed in a systematic way. A simple method which relates the two kinds of phenomena is expected to contribute to our insight into growth processes.

The complex behaviour of dynamical systems can be described by attractors [15] which are objects embedded in a relatively low-dimensional phase and have a fractional dimension [12, 16, 17]. From the experimental point of view, the complexity of the temporal behaviour is usually examined using the measured time series of a scalar quantity. In particular, one can determine the power spectrum of the signal and construct various plots from the time-delayed data [18]. In the case of delaying m times, one obtains a set of points in the d_m-dimensional space whose correlation dimension [17] is an important characteristic of the dynamics.

The main questions addressed in this letter are the following. How can one establish an *analogy* between the experimentally seen complex behaviours in time and space? What is the *degree of randomness* of patterns growing deterministically? In order to treat the above problems we shall use an approach which relates patterns to time series. This method is expected to be useful since during the past decade powerful methods have been elaborated for the treatment of chaotic signals observed as a function of time in chaotic systems.

Our final goal is to investigate the above questions in the context of *interfacial growth* under essentially deterministic conditions. This can be carried out by characterising the geometry of disordered patterns evolving in two-phase fluid flows. Fluid flows are known to exhibit several kinds of instabilities which are described by the Navier-Stokes equation. When one is interested in the dynamic behaviour of the flows, one can use a detector at a fixed point in space and record the velocity-dependent signal as a function of time. Above a critical value of the Reynolds number the signal becomes stochastic indicating the onset of chaos.

Let us develop a similar framework for the investigation of viscous fingering patterns which are also determined by the Navier–Stokes equation with the appropriate boundary conditions. The phenomenon of viscous fingering takes place when a less viscous fluid is injected into a more viscous one under circumstances leading to a fingered interface. The cell consists of two transparent plates of linear size w separated by a relatively small distance b (typical sizes are in the region $w \sim 30$ cm and $b \sim 1$ mm). The viscous fluids are placed between the plates and pressure is applied at the centre of the upper plate (radial cell). Under such conditions the pressure distribution in the incompressible fluids is determined by the Laplace equation [9]

$$\nabla^2 p = 0. \qquad (1)$$

The traditional experiment is carried out using two immiscible, Newtonian fluids with a high viscosity ratio. In the radial Hele–Shaw cell no steady-state fingers can develop because of the Mullins–Sekerka instability [19] which leads to the growth of disordered interfaces shown in figure 1(a) even for low Reynolds numbers.

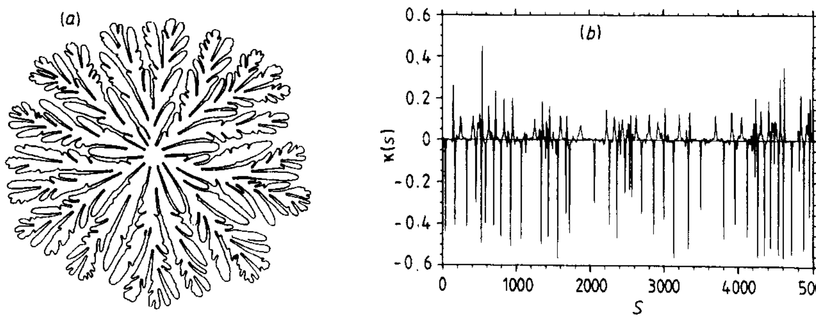

Figure 1. (a) Interface of a representative viscous fingering pattern obtained in the radial Hele–Shaw cell containing glycerin for relatively large pressure of the injected air. (b) Part of the long series of curvature values (5000 out of 38 200) determined for pattern (a) as a function of the arc length.

To characterise the patterns in the thermodynamic limit [20] we determine $\kappa(s)$ which is the local curvature of the interface as a function of the arc length s (distance measured along the surface). Higher-order derivatives could also be used, but the slope of the experimental curves would diverge at many places. In the following, $\kappa(s)$ will be used as an *analogue of the time series* measured in the experiments on dynamical systems.

This approach allows for the following classification of the spatial configurations arising from a simple, but irregular, initial interface.

(i) If the less viscous fluid is drained out from the cell (suction), the interface is stable and the resulting pattern is a circle. Let us now construct a plot of $\kappa(s+\Delta s)$ against $\kappa(s)$ in a manner similar to that used in the theory of chaos to find attractors from a single time series. For a circle we obtain a single point in analogy with the *fixed points* defined for dynamical systems.

(ii) Injecting the less viscous fluid into a system with anisotropy the situation changes qualitatively [21, 22]. In this case nearly periodic, dendritic structures are observed in the vicinity of the tips which are stabilised by the anisotropy. This behaviour in a crude approximation corresponds to a *limit cycle* in the $\kappa(s+\Delta s)$ against $\kappa(s)$ plot.

(ii) Injecting the less viscous fluid into a cell with no anisotropy one obtains patterns without any apparent symmetry. Accordingly, the data seem to be randomly scattered in the related plot of κ values. For recursively constructed fractal curves such as the Koch curve (with a lower cut-off length scale or rounded corners) the curvatures represent a series of numbers (symbols) taking on a few values only and accordingly, the attractor is trivial. This is a qualitatively different case, and it could be treated in a similar framework using an analogy with symbol sequence analysis.

The fractal dimension of patterns and that of the attractor corresponding to the curvature series are not related, these two quantities represent different characteristics of the interfaces. Depending on the level of their randomness, patterns having the same fractal dimension D may have attractors of very different dimensions in the length-shifted phase space (see the above comment on the Koch curve), while the reverse statement is expected to be valid as well. In this sense $\kappa(s)$ discriminates differently created curves in the same manner as D. To get additional information about our viscous fingering patterns the fractal dimension of the interface has been independently determined using the standard box counting method. The result is $D \simeq 1.64$ and the details of the related calculations will be published separately [23].

Of course, the statement relating to the deterministic nature of viscous fingering is only valid if the flow is not dominated by the small random disturbances during the experiments. We carried out the experiments using high quality float glass plates whose irregularities were smaller than 0.01% of the distance between the plates. Gaseous nitrogen was injected, from a large buffer of constant pressure, into glycerin in a regime corresponding to laminar flow. Under such conditions, but in somewhat different geometry, deterministically behaving patterns have been observed in several experiments on viscous fingering [22]. As we shall see later, our data (for the power spectrum and the correlation integral) indicate that the disordered fingering patterns are essentially not completely random. A typical pattern is shown in figure 1(a).

In order to extract quantitative information from the experimental patterns the local curvature, $\kappa(s)$, was determined as a function of the arc length at each pixel point of the digitised image. We achieved a resolution of 1400×1400 pixels by digitising parts of the interface separately. The κ values were obtained by fitting a third degree polynomial to the digitised interface optimising the length of the interval on which the fitting was carried out. We tested the accuracy of our method by calculating κ for circles of various radii and found that down to radii corresponding to about 50 pixels, the systematic error is within 7%. Then the obtained set of approximately 40 000 data was treated as a 'time series'. Figure 1(b) shows part of the long series of data for $\kappa(s)$. The tips of the fingers and the relatively sharp corners at the inner ends of fjords appear as peaks distributed in an apparently random manner. Accordingly, the *power spectrum* of our data has no well defined, singular peaks which would correspond to periodic behaviour. Instead, its decay is approximately exponential for intermediate values of the frequency indicating the deterministic nature of the interface ([24] and references therein).

In search for an underlying structure behind the seemingly stochastic behaviour one can apply a technique analogous to the construction of 'time-delayed' plots. In our case this means plotting the data as points in a d_m-dimensional 'phase' space using the curvature values obtained for the arc lengths $s, s+\Delta s, \ldots, s+(d_m-1)\Delta s$ as coordinates. (In the $d_m = 1$ case the correlations are calculated between the scalar curvature values distributed on an interval.) According to our results for $d_m = 2$ and 3, the data points $\boldsymbol{\kappa}_s = \{\kappa(s), \ldots, \kappa[s+(d_m-1)\Delta s]\}$ are scattered randomly in such *length-shifted* plots. The distribution of points shows no signs of the presence of an attractor corresponding to a low-dimensional spatial chaos.

The degree of randomness can also be examined by estimating the *correlation dimension* D_2 associated with the length shifted set of $\boldsymbol{\kappa}_s$ data. As in the theory of dynamical systems, we expect that with growing d_m the correlation dimension converges to a finite value if the behaviour of the system can be described in terms of a finite-dimensional chaos. The dimension at which this convergence is completed is called the embedding dimension (d_e). For a completely random set of points, i.e. for points produced by a random number generator, $D_2 = d_m$ for all d_m, while, in turn, $D_2 < d_m$ indicates an underlying structure in the data. To determine D_2 one calculates the correlation function $c(r)$ from the expression [18]

$$c(r) = \frac{1}{n^2}[\text{number of pairs of points } (s, s') \text{ with } |\boldsymbol{\kappa}_s - \boldsymbol{\kappa}_{s'}| < r] \qquad (2)$$

and uses the relation

$$c(r) \sim r^{D_2} \qquad (3)$$

where r is supposed to be small.

Using the curvature data obtained for the pattern in figure 1(a) we determined $c(r)$ for various d_m and Δs. A typical set of curves is displayed in figure 2. As for other values of Δs, no well defined, unique slope can be observed in the log-log plots of $c(r)$ (although the slopes of the curves do not seem to saturate for $d_m \leq 10$, their values appear to be smaller than the embedding dimension). One of the conclusions one can draw from this figure is that the structure of our data is very similar to that of a completely random set of points. This is a rather unexpected result because of the simple structure of the equations describing the development of the interface.

In addition, we have also analysed our data using the following method. We have determined the quantity $\delta(r) = \ln c_R(r) - \ln c(r)$, where $\ln c_R$ denotes the correlation

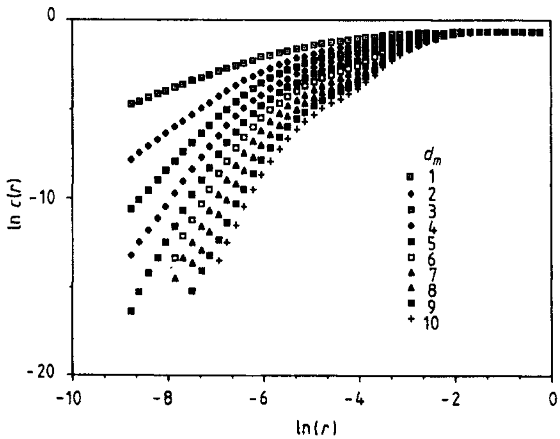

Figure 2. The correlation integral $c(r)$ for the shift parameter value $\Delta s = 10$ and for various trial dimensions d_m. The $d_m = 1$ case corresponds to the correlations between the unshifted data.

integral corresponding to the data set obtained by mixing our original data in a random manner. Our results for $\delta(r)$ and its derivative are shown in figure 3. This figure indicates that $\delta(r)$ scales in a non-trivial way. For completely random original data $\delta(r)$ would remain approximately zero in the scaling region, while in the presence of a low-dimensional attractor the slopes of the curves would change with the trial embedding dimension as $d_m - D_2$ for $d_m \geqslant d_e$. The inset in figure 3 shows that none of these seems to be the case, although our data are quite scattered for obtaining well defined estimates for the local slopes.

The reason for the stochastic behaviour investigated in this letter is the instability of the interface: perturbations beyond a surface tension-dependent wavelength grow indefinitely. These perturbations are present in the *initial condition*, i.e. the starting shape of the interface is never perfectly symmetric. We suggest that the nonlinear mixing of the many Fourier modes of the initial interface produces high-dimensional behaviour. In the absence of stabilising effects (e.g. anisotropy), there is no mechanism which would drive the system into any of the regular shapes. Note that in systems with low-dimensional temporal chaos the onset of chaotic behaviour usually takes place as one of the parameters of the system is changed. In our case the role of this parameter is possibly played by the anisotropy.

In conclusion, applying the techniques widely used for the description of temporal chaos, we have demonstrated the non-existence of an attractor having a simple structure associated with the spatial behaviour of viscous fingering patterns. This fact indicates that in spite of their deterministic origin, growing Laplacian interfaces cannot be described in terms of low-dimensional chaos; instead, they have been found to correspond to a stochastic behaviour of higher degree in space. Finally, the approach presented in this letter can be applied to many other kinds of pattern forming systems and to the characterisation of interfacial structures in general. For instance, implementing the existing algorithms [25] for dynamical systems, it should be straightforward to calculate the related Lyapunov exponents for patterns corresponding to low-dimensional chaos.

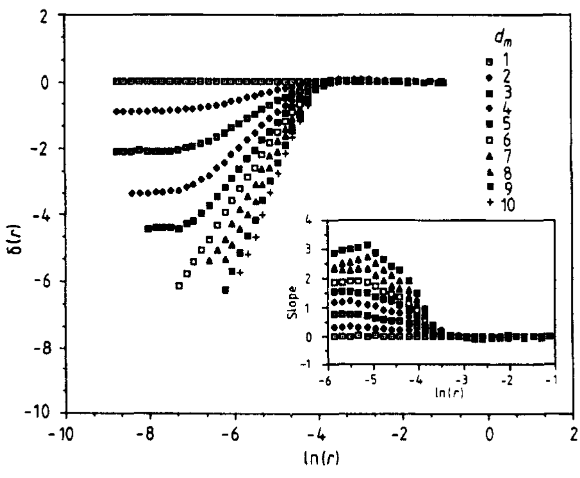

Figure 3. The difference $\delta(r)$ for $\Delta s = 10$ between the correlation integral $c_R(r)$ calculated for the data set obtained by randomly mixing the original curvature values and the correlation integral $c(r)$ corresponding to the original $\kappa(s)$ series. The inset shows the derivatives obtained for the plots displayed in the main part of the figure.

We thank G Bene, G Györgyi, J Kertész, P Szépfalusy, T Tél and K Wiesenfeld for useful discussions.

References

[1] Meakin P 1987 *Phase Transitions and Critical Phenomena* vol 12, ed C Domb and J L Lebowitz (New York: Academic) p 365
[2] Stanley H E and Ostrowsky N (eds) 1988 *Random Fluctuations and Pattern Growth* (Dordrecht: Kluwer)
[3] Vicsek T 1989 *Fractal Growth Phenomena* (Singapore: World Scientific)
[4] Witten T A and Sander L M 1981 *Phys. Rev. Lett.* **47** 1400
[5] Forrest S R and Witten T A 1979 *J. Phys. A: Math. Gen.* **12** L109
[6] Brady R M and Ball R C 1984 *Nature* **309** 225
Matsushita M, Sano M, Hayakawa Y, Honjo H and Sawada Y 1984 *Phys. Rev. Lett.* **53** 286
[7] Radnóczy Gy, Vicsek T, Sander L M and Grier D 1987 *Phys. Rev.* A **35** 4012
[8] Niemeyer L, Pietronero L and Wiesmann H J 1984 *Phys. Rev. Lett.* **52** 1033
[9] Paterson L 1981 *J. Fluid Mech.* **113** 513
Bensimon D, Kadanoff L P, Liang S, Shraiman B I and Tang L 1986 *Rev. Mod. Phys.* **58** 977
[10] Maloy K J, Feder J and Jossang J 1986 *Phys. Rev. Lett.* **55** 2681
[11] Daccord G, Nittmann J and Stanley H E 1986 *Phys. Rev. Lett.* **56** 336
[12] Mandelbrot B B 1982 *The Fractal Geometry of Nature* (San Francisco: Freeman)
[13] Feder J 1988 *Fractals* (New York: Plenum)
[14] Sander L M, Ramanlal P and Ben-Jacob E 1985 *Phys. Rev.* A **32** 3160
[15] Eckmann J P and Ruelle D 1985 *Rev. Mod. Phys.* **57** 617
Swinney H L and Gollub J P (eds) 1985 *Hydrodynamic Instabilities and the Transition to Turbulence* (Berlin: Springer)
Berge P, Pomeau Y and Vidal C 1986 *Order Within Chaos* (New York: Wiley)
[16] Farmer J D, Ott E and Yorke 1983 *Physica* **7D** 153
[17] Grassberger P and Procaccia I 1983 *Phys. Rev. Lett.* **50** 346
[18] Takens F 1981 *Dynamical Systems and Turbulence* ed D Rand and L S Yung (Berlin: Springer)
Packard N H, Crutchfield J P, Farmer J D and Show R S 1983 *Phys. Rev. Lett.* **45** 712
[19] Mullins W W and Sekerka R F 1963 *J. Appl. Phys.* **34** 323
[20] Rauseo S N, Barnes P D and Maher J V 1987 *Phys. Rev.* A **35** 1245
[21] Ben-Jacob E, Godbey Y, Goldenfeld N, Koplik J, Levine H, Mueller T and Sander L M 1985 *Phys. Rev. Lett.* **55** 1315
Buka A, Kertész J and Vicsek T 1986 *Nature* **323** 424
[22] Park C W and Homsy G M 1985 *Phys. Fluids* **28** 1583
Couder Y, Cardoso O, Dopuy D, Tavernier P and Thom W 1986 *Europhys. Lett.* **2** 437
[23] Horváth V K to be published
[24] Brandstater A and Swinney H L 1987 *Phys. Rev.* A **35** 2207
[25] Sano M and Sawada Y 1985 *Phys. Rev. Lett.* **55** 1082
Eckmann J P, Kamphorst S O, Ruelle D and Ciliberto S 1986 *Phys. Rev.* A **34** 4971